Studies of CO Adsorption on Pt(100), Pt(410), and Pt(110) Surfaces Using Density Functional Theory

Shuichi Yamagishi,[†] Toshiyuki Fujimoto,[†] Yasuji Inada,[‡] and Hideo Orita*[,†]

National Institute of Advanced Industrial Science and Technology (AIST), Tsukuba Central 5, 1-1-1 Higashi, Tsukuba, Ibaraki 305-8565, Japan, and Accelrys K. K., Nishishinbashi TS Building, 3-3-1 Nishishinbashi, Minato-ku, Tokyo 105-0003, Japan

Received: February 10, 2005; In Final Form: February 16, 2005

Adsorption of CO on Pt(100), Pt(410), and Pt(110) surfaces has been investigated by density functional theory (DFT) method (periodic DMol[3]) with full geometry optimization and without symmetry restriction. Adsorption energies, structures, and vibrational frequencies of CO on these surfaces are studied by considering multiple possible adsorption sites and comparing them with the experimental data. The same site preference as inferred experiments is obtained for all the surfaces. For Pt(100), CO adsorbs at the bridge site at low coverage, but the atop site becomes most favorable for the $c(2 \times 2)$ structure at 1/2 monolayer. For Pt(410) (stepped surface with (100) terrace and (110) step), CO adsorbs preferentially at the atop site on the step edge at 1/4 monolayer, but CO populates also at other atop and bridge sites on the (100) terrace at 1/2 monolayer. The multiple possible adsorption sites probably correspond to the multiple states in the temperature-programmed desorption spectra for CO desorption. For Pt(110), CO adsorbs preferentially at the atop site on the edge for both the reconstructed (1×2) and the un-reconstructed (1×1) surfaces. When adjacent sites along the edge row begin to be occupied, the CO molecules tilt alternately by ca. 20° from the surface normal in opposite directions for both the (1×2) and (1×1) surfaces.

1. Introduction

The interaction of CO with metal surfaces has been studied extensively with great academic and industrial interest because it is an indispensable step in surface and catalytic reactions such as CO oxidation and hydrogenation. An understanding of chemisorption and heterogeneous catalysis on metal surfaces requires a detailed knowledge of adsorbate structure with respect to the substrate. Structure sensitivity is another interesting topic of surface science and catalysis.[1,2] Heats of adsorption and local bonding geometries have been investigated not only experimentally but also theoretically.[3,4] However, there is a puzzling problem, that density functional theory (DFT) tends to predict the wrong adsorption site such as the fcc-hollow site, whereas the atop site is preferred experimentally for CO on Pt surfaces. Feibelman et al.[5] have performed a comprehensive study of this problem by using different plane-wave-based DFT computational codes. They have concluded that DFT at the generalized gradient approximation (GGA) level tends to favor a higher coordination site, which is correct in the case of Ni(111) and Pd(111), but incorrect in the case of Pt(111) where the atop site is preferred. They have obtained a preference of at least 0.10 eV for the fcc site above the atop site. Previously, we have investigated adsorption of CO on Pt(111) by a periodic DFT method with full geometry optimization, changing calculation parameters (core treatment, functional, number of slab layer, *k*-points, Fermi smearing, and size of the unit cell)[6] and compared previous results in the literature. We have found that all electron scalar relativistic (AER) calculations are essential to obtain the correct site preference, atop followed by bridge and hollow (fcc and hcp). The energy difference between the atop and bridge sites is 0.09 eV and corresponds well to the recent reanalyzed value of the experimental data of 0.095 ± 0.015 eV.[7] The AER calculations give a deeper Fermi level for a Pt surface with all the functionals, which provides the effect for decreasing the interaction of the LUMO (lowest unoccupied molecular orbital) of CO with the metal substrate and leads to the correct site preference. The relative energetic ordering and site preference are not dependent on functionals, although the absolute adsorption energy is varied by functionals and somewhat overestimated. The overestimation of adsorption energy is the general trend in the present DFT methods (e.g., see refs 3 and 8−10), and recently Mason et al.[10] have proposed an extrapolation correction method for adsorption energies. The convergence of the relative energy difference among the sites is within 0.02 eV when using the same core treatment and functional,[6] so the relative energy difference among the sites becomes the most important parameter for comparing the properties of adsorption sites.

Extending the work on Pt(111), we have been continuously undertaking an extensive investigation of CO adsorption on Pt surfaces to study the structure sensitivity of CO adsorption. Some results on Pt(211) and Pt(311) have been already published,[11] and the results on Pt(100), Pt(410), and Pt(110) surfaces are reported in the present paper. The characteristic features of these three surfaces are as follows. A clean Pt(100) surface is reconstructed in the (5×20) structure normally referred to as the hex phase and reverts to the (1×1) structure during adsorption of CO.[3,12−14] The (410) surface consists of four-atom-wide terraces with (100) structure and one-atom-high steps with (110) character. The (100) and (110) microfacets decline from the macroscopic (410) surface plane by +14.0 and

* To whom correspondence should be addressed. Phone: +81-29-861−-4835. Fax: +81-29-861-9291. E-mail: hideo-orita@aist.go.jp.
[†] AIST.
[‡] Accelrys K. K.

10.1021/jp050722i CCC: $30.25
Published on Web 03/30/2005

−31.0°, respectively. A clean surface of Pt(110) is also reconstructed to the (1 × 2) phase with a missing row, and the adsorption of CO leads to lifting of this reconstruction to the (1 × 1) phase.[15,16]

Previous calculations for CO on Pt surfaces[5,9,17−20] except ours[6,11] cannot obtain the same site preference as inferred experiments; i.e., the hollow or bridge site is most favorable theoretically, whereas the atop site is preferred experimentally. We have investigated adsorption energies and structures of CO on the above three Pt surfaces with full-geometry optimization and without symmetry restriction and compared them with the experimental data. We have obtained the same site preference as inferred experiments on all three surfaces and can assign the peaks of C−O stretching vibration very well.

2. Computational Methods

DFT calculations were performed with the program package DMol[3] in Materials Studio (version 2.2) of Accelrys Inc. on personal computers. In the DMol[3] method,[21−23] the physical wave functions are expanded in terms of accurate numerical basis sets. We used the double-numeric quality basis set with polarization functions (DNP). The size of the DNP basis set is comparable to Gaussian 6-31G**, but the DNP is more accurate than the Gaussian basis set of the same size. The gradient-corrected GGA functional, developed by Perdew, Burke, and Ernzerhof (PBE),[24] was employed. A Fermi smearing of 0.002 hartree (1 hartree = 27.2114 eV) and a real-space cutoff of 4 Å were used to improve computational performance. Periodic surface slabs of four layers' thickness were used, with a 10 Å of vacuum region between the slabs. Adsorbate and the two top layers of metal were allowed to relax in all the geometry optimization calculations without symmetry restriction (i.e., always using P1 symmetry). The tolerances of energy, gradient, and displacement convergence were 2×10^{-5} hartree, 4×10^{-3} hartree/Å, and 5×10^{-3} Å, respectively. The maximum gradient for most of the optimized structures was less than 2×10^{-3} hartree/Å. Adsorption energies were computed by subtracting the energies of the gas-phase CO molecule and surface from the energy of the adsorption system, as shown in

$$E_{ad} = E(\text{CO/surface}) - E(\text{CO}) - E(\text{surface}) \qquad (1)$$

With this definition, a negative E_{ad} corresponds to stable adsorption on the surface.

The experimentally determined Pt lattice constant of 3.924 Å was used for the production of the surfaces. All electron scalar relativistic (AER)[25] calculations were performed, since we have shown in the previous work on CO on Pt(111)[6] that AER calculations were essential to obtain the same site preference as inferred in experiments. Delley has reported an error for Pt bulk lattice constant as −0.41%.[26] Gil et al.[27] have checked the effect of using the experimental lattice constant, instead of the commonly used optimized value for the bulk. They have concluded that there is no significant effect on the difference in adsorption energy between atop and hollow sites. For the numerical integration, we used the XFINE quality mesh size of the program, which is a nearly saturated mesh for benchmark calculations. The tolerance of SCF convergence was 1×10^{-7}. Under the present computational conditions, the C−O bond length for free CO molecule was calculated as 1.14 Å, in good agreement with the experimental value of 1.13 Å.[28] The bond energy was calculated as 11.97 eV. The value also agrees well with the reported one (11.66 eV) of Kurth and co-workers.[29]

Harmonic vibrational frequencies were calculated with displacing not only the CO molecules but also the first layer Pt atoms of surfaces as described in detail previously.[30] To reduce the computationally expensive cost of frequency calculation, density functional semicore pseudopotentials (DSPPs)[26] were employed instead of AER for AER-geometry-optimized structures. Under the present calculational conditions, the harmonic frequency of free CO molecule (d(C−O) = 1.14 Å) was calculated as 2127 cm^{-1}. This value is 2.0% smaller than the experimental harmonic value of 2170 cm^{-1}, and much closer to the anharmonic one (2143 cm^{-1}).[28]

For Pt(100), an un-reconstructed $p(2 \times 2)$ surface unit cell (including 16 Pt atoms) was chosen to model adsorption of CO for a low coverage of 1/4 monolayer and a $c(2 \times 2)$ ordered structure (1/2 monolayer: two CO molecules in the $p(2 \times 2)$ unit cell). A $5 \times 5 \times 2$ k-point sampling was used. Although the clean Pt(100) surface is reconstructed, CO adsorption leads to a lifting of this reconstruction to a (1 × 1) structure.[3,12−14,31,32] Therefore, only the un-reconstructed surface is considered in the present work. Three adsorption sites (atop, bridge, and hollow) were investigated by attaching the carbon atom of CO to the surface.

For Pt(410), a (1 × 1) surface unit cell (including 16 Pt atoms) was chosen to model adsorption of CO for coverages of 1/4 and 1/2 monolayer. A $3 \times 5 \times 1$ k-point sampling was used. First, 10 adsorption sites shown in Figure 1 were investigated at the coverage of 1/4 monolayer. Second, four different configurations of the adsorbed CO were investigated at the coverage of 1/2 monolayer by considering the sum of adsorption energies for single adsorption and local geometries between the CO adsorbates.

For Pt(110), a clean surface is reconstructed with a missing row, and the adsorption of CO leads to lifting of Pt surface to an un-reconstructed phase.[15,16] However, since the reconstruction remains due to the immobility of the Pt atoms below 250 K, it is possible to study the adsorption of CO on the "frozen-in" reconstructed phase.[33] Therefore, we adopted two models which are a reconstructed missing row phase and an un-reconstructed phase. A reconstructed missing row (2 × 2) surface unit cell (including 32 Pt atoms) was chosen to model adsorption of CO on the reconstructed surface with the coverages of 1/8 and 1/4 monolayer. A $4 \times 3 \times 1$ k-point sampling was used. Nine adsorption sites shown in Figure 2 were investigated. On the other hand, an un-reconstructed (2 × 1) surface unit cell (including 16 Pt atoms) was chosen to model adsorption of CO on the un-reconstructed surface with the coverages of 1/4 and 1/2 monolayer. A $4 \times 5 \times 1$ k-point sampling was used. Only four adsorption sites shown in Figure 3 were investigated.

3. Results and Discussion

3.1. Pt(100). Although adsorption of CO on Pt(100) is a well-studied system, considerable confusion exists especially over the vibrational data (see ref 13). To remove the inconsistencies arising from previous studies, Martin et al.[13] have studied adsorption on both the reconstructed and the metastable un-reconstructed surfaces carefully at temperatures between 90 and 300 K. They have found that on the un-reconstructed surface at 90 K initial CO exposure results in a single bridge band at 1874 cm^{-1}, and an atop band grows at 2075 cm^{-1} after further exposure. They have concluded that the ratio of bridge to atop site occupancy is coverage-dependent and that the $c(2 \times 2)$ structure corresponds to a mixture of domains of all-bridge or all-atop species, but the relative proportions of each varies as a function of temperature with bridge domains favored at 90 K. When the coverage exceeds 1/2 monolayer, the coverage-dependent behavior of CO adsorption becomes much more

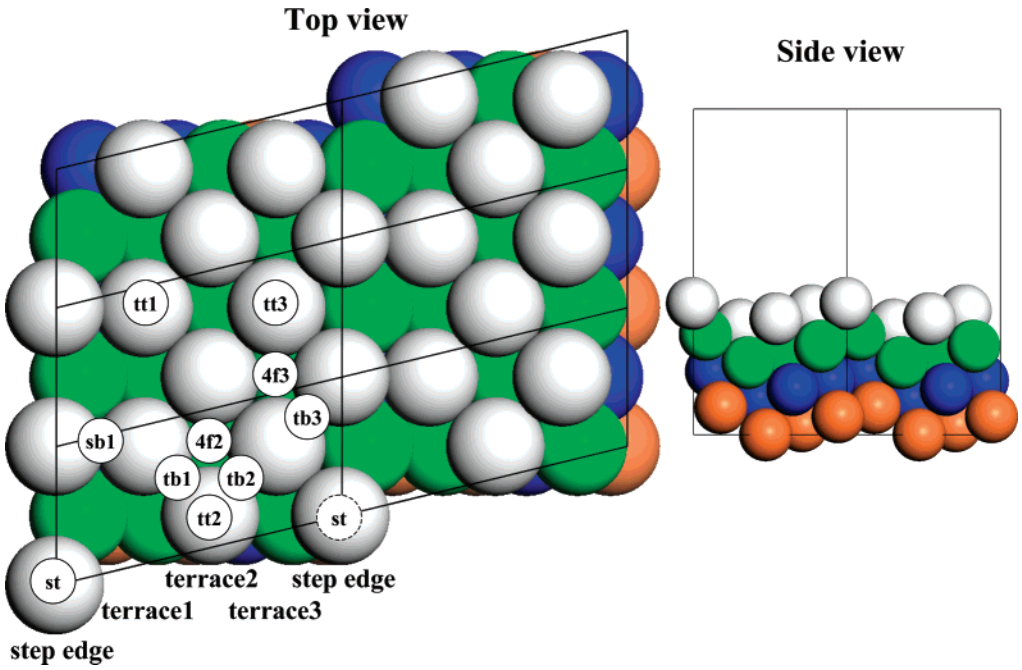

Figure 1. (Left) Illustration of adsorption sites on the (410) surface in the top view with the (1 × 1) unit lattice. The metal rows on the surface are classified into four types of step edge, terrace1, terrace2, and terrace3 by coordinate numbers of 6, 9, 8, and 8, respectively. Adsorption sites are abbreviated as follows: st, atop site on step edge; sb1, bridge site perpendicular to step edge; tt1, atop site on terrace1 (terrace1 refers to the terrace near the step bottom); tb1, bridge site between terrace1 and terrace2 (terrace2 refers to the terrace going further from terrace1 to the step edge); tt2, atop site on terrace2; 4f2, 4-fold hollow site among terrace1, terrace2, and terrace3; tb2, bridge site between terrace2 and terrace3 (terrace3 refers to the terrace near the step edge); tt3, atop site on terrace3; 4f3, 4-fold hollow site among terrace2, terrace3, and the step edge; tb3, bridge site between terrace3 and the step edge. (Right) Side view of the (410) surface with the unit lattice.

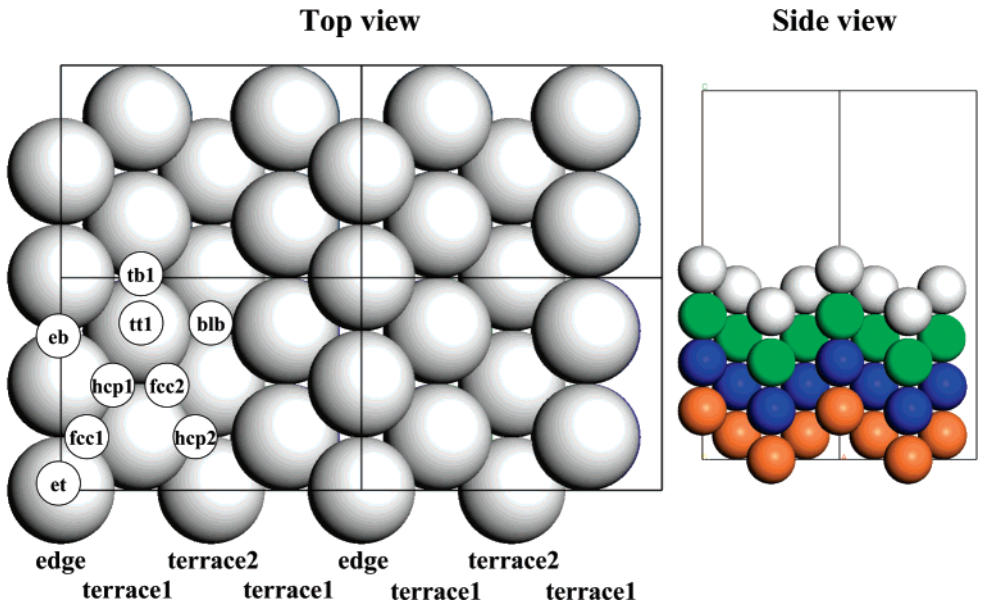

Figure 2. (Left) Illustration of adsorption sites on the reconstructed missing row (110) surface with the (2 × 2) unit lattice. The metal rows on the surface are classified into three types of edge, terrace1, and terrace2 by the coordinate numbers of 7, 9, and 11, respectively. Adsorption sites are abbreviated as follows: et, atop site on the edge; eb, bridge site parallel to the edge; fcc1, fcc hollow site between the edge and terrace1 (terrace1 refers to the terrace near the edge); hcp1, hcp hollow site between the edge and terrace1; tt1, atop site on terrace1; tb1, bridge site between two terrace1 atoms; fcc2, fcc hollow site between terrace1 and terrace2 (terrace2 refers to the terrace at the bottom); hcp2, hcp hollow site between terrace1 and terrace2; blb, long-bridge site at the bottom. (Right) Side view of the reconstructed missing row (110) surface with the unit lattice.

complex, and a sequence of ordered overlayers is observed. Therefore, we have concentrated in the present work on calculating adsorption energies and structures of CO on the unreconstructed surface of Pt(100) at the two different coverages of 1/4 and 1/2 monolayer in the same $p(2 \times 2)$ unit cell in order to remove an error which might come from using different unit cells. The results are listed in Table 1. Typical optimized adsorption structures for Pt(100) are shown in Figure 4. All the CO molecules adsorb perpendicularly to the surface, and the Pt atoms attaching to CO move upward a little. The most favorite adsorption of 1/4 monolayer coverage occurs at the bridge site with $E_{ad} = -2.27$ eV, but the energy difference from the second favorite site of atop is only 0.05 eV. The CO molecule at the 4-fold hollow site is less stable with $E_{ad} = -1.64$

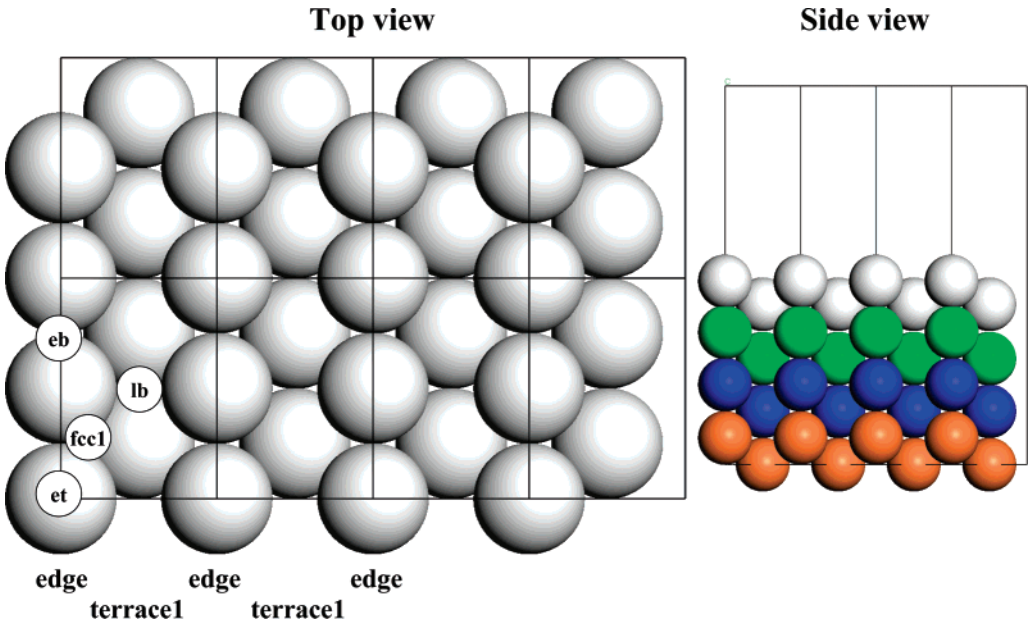

Figure 3. (Left) Illustration of adsorption sites on the un-reconstructed (110) surface with the (2 × 1) unit lattice. The metal rows on the surface are classified into two types of edge and terrace1 by the coordinate numbers of 7 and 11, respectively. Adsorption sites are abbreviated as follows: et, atop site on the edge; eb, bridge site parallel to the edge; lb, long-bridge site at the bottom; fcc1, fcc hollow site between the edge and terrace1. (Right) Side view of the un-reconstructed (110) surface with the unit lattice.

TABLE 1: Adsorption Energies, Structures, and Stretching Frequencies for CO on Pt(100) Surface in a *p*(2 × 2) Unit Cell

ad site	E_{ad}[a]/eV	*d*(Pt−C)[b]/Å	*d*(C−O)[b]/Å	ν(CO)/cm^{-1} (expt)
1/4 monolayer				
atop	−2.22	1.83	1.16	2073 (2075[13])
bridge	−2.27	2.01, 2.01	1.18	1841 (1874[13])
hollow	−1.64	2.27, 2.27, 2.27, 2.27	1.20	1691
1/2 monolayer, *c*(2 × 2) structure				
2 atop	−2.24	1.82, 1.82	1.16, 1.16	2088, 2032 (2088[13])
2 bridge	−2.21	2.01, 2.01, 2.01, 2.01	1.18, 1.18	1879, 1831 (1883[13])
2 hollow		not stable: move to 2 bridge		
free CO			1.14	2127 (2143[28])

[a] Adsorption energy per CO molecule. [b] For reference, the experimental values of *d*(Pt−C) and *d*(C−O) for CO/Pt(111) are 1.85 (atop)/2.08 (bridge) and 1.15 (atop and bridge) Å, respectively.[34]

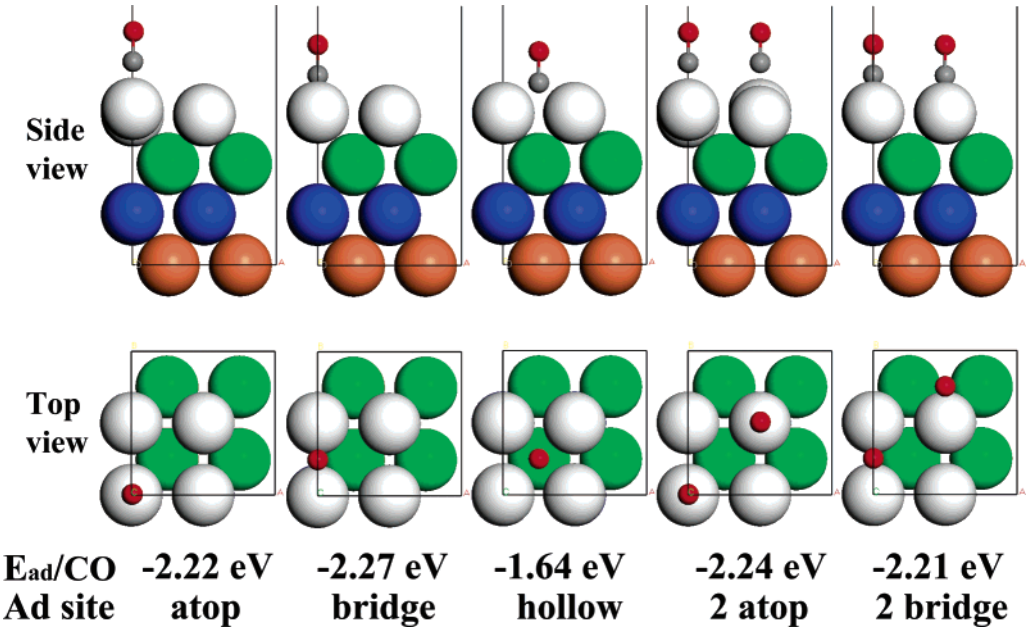

Figure 4. Typical adsorption structures of CO on Pt(100).

eV. Yeo et al.[14] have measured the adsorption heat of CO on the un-reconstructed surface calorimetrically. The initial adsorption heat is 2.33 eV but drops quickly and remains constant at 2.23 eV between 0.05 and 0.25 monolayer. Between 0.25 and 0.5 monolayer, there is a second plateau of adsorption heat at 2.02 eV. The calculated values for the bridge and atop sites are

TABLE 2: Adsorption Energies, Structures, and Stretching Frequencies for CO on Pt(410) Surface in a (1 × 1) Unit Cell

ad site	E_{ad}[a]/eV	d(Pt−C)[b]/Å	d(C−O)[b]/Å	tilt angle[c]/deg	ν(CO)/cm^{-1} (expt)
1/4 monolayer					
st	−2.49	1.84	1.16	−15.9	2063 (2072−2090[37])
tt1		not stable: move to sb1			
tt2	−2.24	1.82	1.16	11.3	
tt3	−2.33	1.82	1.16	9.5	
sb1	−2.23	1.99, 2.00	1.18	-19.7	
tb1	−2.25	1.99, 2.01	1.18	7.2	
tb2	−2.33	2.00, 2.01	1.18	12.5	1857 (1869[37])
tb3	−2.31	1.98, 2.03	1.18	3.4	
4f2		not stable: move to tb2			
4f3		not stable: move to tb3			
1/2 monolayer					
st + tb2	−2.39	st: 1.84	1.16	−18.9	2066, 1848
		tb2: 1.96, 2.02	1.18	12.8	
st + tt2	−2.36	st: 1.83	1.16	−14.9	2081, 2033
		tt2: 1.82	1.16	11.0	
st + tt3	−2.33	st: 1.85	1.16	−25.1	2086, 2038
		tt3: 1.82	1.16	16.7	
st + tb1	−2.32	st: 1.84	1.16	−6.6	2069, 1858
		tb1: 1.99, 2.01	1.18	5.9	

[a] Adsorption energy per CO molecule. [b] For reference, the experimental values of d(Pt−C) and d(C−O) for CO/Pt(111) are 1.85 (atop)/2.08 (bridge) and 1.15 (atop and bridge) Å, respectively.[34] [c] Tilt angle stands for the angle of the C−O axis from the macroscopic (410) normal.

very close to the experimental adsorption heat between 0.05 and 0.25 monolayer. The C−O stretching frequencies are calculated as 2073, 1841, and 1691 cm^{-1} for the atop, bridge, and hollow sites, respectively. The calculated frequencies for the atop and bridge sites also agree well with the experimental ones of Martin et al. at low exposures.[13] By means of the extrapolation correction method,[10] Mason et al. have found that the most stable adsorption at 1/4 monolayer on Pt(100) occurs at the bridge site with $E_{ad} = -1.824$ eV, and that the energy difference between the bridge and atop sites is only 0.028 eV (the difference without correction is 0.185 eV). The corrected energy difference of Mason et al. is similar to ours, although the absolute adsorption energy is a little smaller than ours.

On the other hand, for the $c(2 \times 2)$ structure at 1/2 monolayer, the most favorite adsorption occurs at the atop site with $E_{ad} = -2.24$ eV/CO, although the energy difference from the second favorite site of bridge is only 0.03 eV/CO. The atop and bridge domains are probably populated simultaneously. The 4-fold hollow site becomes unstable at the coverage of 1/2 monolayer, probably because neighboring CO molecules share the Pt atoms. The calculated vibrational frequencies for the atop species of the $c(2 \times 2)$ structure at 1/2 monolayer are 2088 cm^{-1} (symmetric mode and dipole active being visible in IR measurements: two CO molecules vibrate in the same direction) and 2032 cm^{-1} (antisymmetric mode: two CO molecules vibrate in the opposite directions), which is in good agreement with the experimental result of 2088 cm^{-1} at the exposure where the $c(2 \times 2)$ LEED pattern develops its maximum intensity at 300 K. For the bridge site, the frequencies are calculated as 1879 and 1831 cm^{-1}, which also agrees well with the experimental result of 1883 cm^{-1}. The calculated adsorption energies do not include effects of zero-point vibrational energies. Even when considering only the calculated frequencies of C−O stretching vibrations, the energy difference between the atop and bridge domains for the $c(2 \times 2)$ structure at 1/2 monolayer becomes smaller to 0.017 eV/CO. Therefore, the bridge domains are probably more favored at lower temperature. All the results of the present calculation are quite consistent with the experimental ones of Martin et al.[13] and can interpret them very well. The Pt−C and C−O distances for the atop and bridge sites are quite similar to those calculated previously for Pt(111).[6] These distances are in good agreement with the experimental ones for CO on Pt(111) by LEED[34] (Pt−C distance, 1.85 ± 0.1 and 2.08 ± 0.07 Å for the atop and bridge sites, respectively; C−O distance, 1.15 ± 0.05 Å for both sites), although there is no report on the determination of C−O and Pt−C distances for CO on Pt(100).

3.2. Pt(410). Masel and co-workers[35−37] have investigated adsorption and interaction of NO and CO on Pt(410) and found that Pt(410) is an unusually active surface for decomposition of NO and CO. They have observed some evidence for NO decomposition and N_2O formation at 120 K, CO dissociation and carbon deposition at 480 K, and a surface explosion during the NO/CO reaction at 360 K.[36] Banholzer et al.[37] have reported that adsorption of CO on Pt(410) at room temperature gives a single IR band which shifts from 2072 to 2090 cm^{-1} with increasing exposure. This shift can be decomposed into a 36 cm^{-1} upward shift due to dipole/dipole repulsive interactions between adjacent CO molecules on the surface and a 18 cm^{-1} downward shift due to a change in the chemical environment (back-donation of metal d electrons into π^* orbital of CO) on the surface as lower binding states fill. They have also reported that there is a second band at 1869 cm^{-1} after the CO layer is heated or contaminated by carbon, and bands below 2000 cm^{-1} are usually associated with bridge-bound CO, as shown in the previous section. We have calculated the adsorption energies and structures of CO on Pt(410) at the two different coverages of 1/4 and 1/2 monolayer in the (1 × 1) unit cell in order to compare them with the experimental results. The calculated adsorption energies and structures are listed in Table 2, and typical optimized adsorption structures are shown in Figure 5 (other optimized structures are available as Supporting Information). The most favorite adsorption of 1/4 monolayer CO coverage occurs at the st site with $E_{ad} = -2.49$ eV (for abbreviation of adsorption sites, see the caption of Figure 1). The CO molecule tilts away (−15.9°) from the (410) normal to the (110) normal. Since the energy difference from the second favorite sites of tt3 and tb2 is 0.16 eV, the CO molecules at these sites are recognized to be less stable than the CO at the st site. These results agree with those of the experiment performed by Banholzer et al.[37] because their observed CO vibrational frequency (2072−2090 cm^{-1}) shows that CO adsorbs at the atop site of the surface. The CO molecules at the tt2 and tb2 sites, which are located around the center of the terrace,

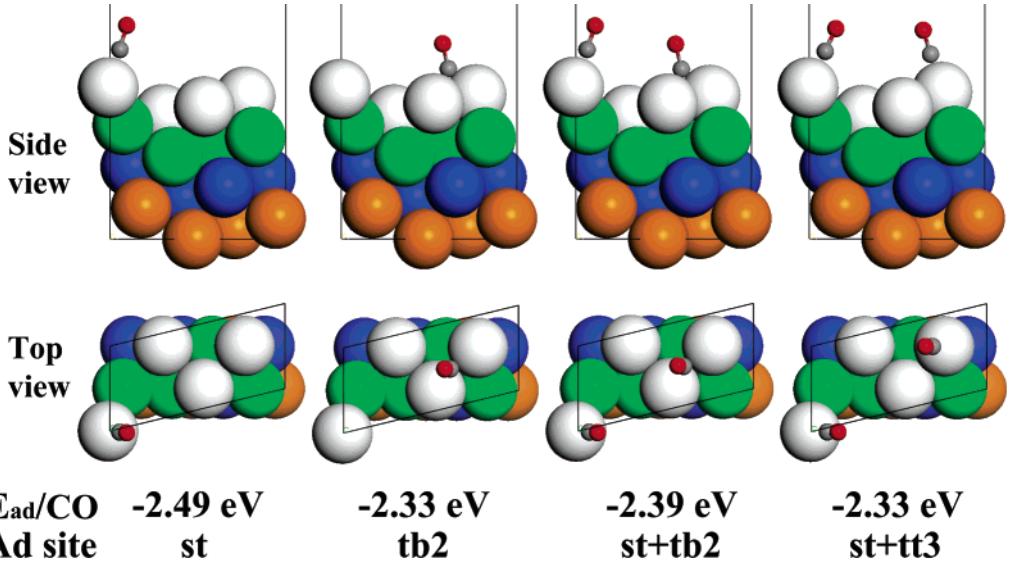

Figure 5. Typical adsorption structures of CO on Pt(410).

adsorb almost parallel to the (100) normal (14.0°). Their Pt−C and C−O distances are the same as those for the CO molecules on Pt(100) (cf. Table 1). The 4-fold hollow sites are not stable, and the CO molecules move to neighboring bridge sites.

The most stable adsorption configuration at 1/2 monolayer is st + tb2 with $E_{ad} = -2.36$ eV/CO, but the energy difference from the second favorite adsorption configuration of st + tt2 is only 0.03 eV/CO. The energy differences from the third and fourth favorite adsorption configurations are also small at 0.06 and 0.07 eV/CO, so these four configurations are populated simultaneously at 1/2 monolayer. These multiple possible adsorption configurations probably correspond to the multiple states in the temperature-programmed desorption (TPD) spectra for CO desorption from Pt(410) observed by Park et al.,[36] but clear assignment is not possible because the surface condition is changing during TPD ramp due to CO dissociation or surface reconstructions (see ref 36 for detailed discussion).

To compare with the experimental vibrational frequencies of Banholzer et al.,[37] harmonic vibrational frequencies are calculated for the st + tb2 configuration. Two C−O stretching frequencies are obtained as 2066 and 1848 cm^{-1}. The higher and lower frequencies originate mainly for the CO molecules at the st and tb2 sites, respectively. To check if the vibrational coupling of the st and tb2 CO molecules is weak, we have also calculated vibrational frequencies for the st and tb2 species independently. The frequencies are obtained as 2063 and 1857 cm^{-1} for the st and tb2 species, respectively. The difference of frequencies is only up to 9 cm^{-1}. The calculated frequencies are in reasonable agreement with the experimental ones, although the bridge band is only seen after a CO layer is heated or contaminated by carbon in the experiment of Banholzer et al.,[37] where adsorption is carried out only above room temperature. Lower temperature may be needed to populate adsorption configurations at higher coverage of 1/2 monolayer. There is considerable confusion on observing bridge C−O band on Pt surfaces (e.g., Pt(100),[13] Pt(533),[38] and Pt(211)[39]), mainly due to a relatively small intensity and the large broadness of the bridge band. The appearance of the bridge band is also influenced easily by the cleanness of surfaces, as discussed by Banholzer et al.[37] We have also calculated the C−O stretching frequencies for the other three configurations at 1/2 monolayer. For the two atop configurations (i.e., st + tt2 and st + tt3), the frequencies are obtained as 2081 (symmetric and dipole active mode) and 2033 (antisymmetric mode) cm^{-1}, and 2086 (symmetric) and 2038 (antisymmetric) cm^{-1}, respectively. When these configurations are populated, the C−O frequencies shift to higher wavenumber, as observed by Banholzer et al.[37] For the st + tb1 configuration, the frequencies are 2069 and 1858 cm^{-1}. All the calculated frequencies also agree well with the experimental ones of Banholzer et al.[37]

3.3. Pt(110). It is well-known that a clean surface of Pt(110) is reconstructed to the (1 × 2) phase with a missing row and the adsorption of CO leads to lifting of the Pt surface to the (1 × 1) phase.[15,16] Hofmann et al. have reported in their earlier paper on CO/Pt(110)[40] that CO is adsorbed into atop sites at all coverages as inferred from HREELS, but they have later reported the coexistence of the bridge CO species by adsorption at lower temperature[41] and upon partial desorption from the (2 × 1)-p1g1-CO structure.[42] Sharma et al. have found by means of reflection adsorption infrared spectroscopy (RAIRS)[33] that CO occupies atop sites exclusively at all coverages and temperatures and that no large C−O frequency change is seen when the (1 × 2) reconstructed surface phase converges to the (1 × 1) surface phase. The lifting of the reconstruction is dependent on both surface temperature and adsorbate coverage, and the (1 × 2) reconstruction remains due to the immobility of the Pt atoms below 250 K. Therefore, it is possible to study the adsorption of CO on the "frozen-in" (1 × 2) phase. At 90 K, below 0.2 langmuir, the single band at ca. 2064 cm^{-1} is assigned to isolated upright CO adsorbed at atop sites along the [110] row because of no lateral repulsion between neighboring molecules. However, as the dose increases, a high-frequency shoulder appears at 2095 cm^{-1}, which dominates at saturation due to extensive dipole coupling of CO. When adjacent sites along the row begin to be occupied, a two-phase system forms: an island of tilted atop CO coexisting with upright atop CO along the [110] rows.[33] By combining the angle-resolved UV photoelectron spectroscopy (ARUPS) experiments with increasing coverage of CO on the surface, Hofmann et al.[41] have estimated the tilting of CO molecules by ca. 15° from the surface normal in opposite directions on the reconstructed (1 × 2) surface at saturation coverage with simultaneous observation of the bridge species at 1855 cm^{-1}. Freyer et al. also have observed a sequential adsorption into atop and bridge sites on the reconstructed (1 × 2) surface at 120 K, yielding an ordered $c(8 \times 4)$ structure without the lifting of the reconstruction.[43]

TABLE 3: Adsorption Energies, Structures, and Stretching Frequencies for CO on the Pt(110) Surface in Reconstructed Misssing Row (2 × 2) and Un-reconstructed (2 × 1) Unit Cells

ad site	E_{ad}[a]/ eV	d(Pt−C)/Å (expt)[c]	d(C−O)/Å (expt)[c]	tilt angle[b]/deg (expt)[c]	ν(CO)/cm^{-1} (expt)[c]
		Reconstructed Missing Row (2 × 2)			
1/8 monolayer					
et	−2.36	1.84 (1.9[48])	1.16 (1.3[48])	0.4 (0.0[40])	2055 (2058−2064[33])
eb	−2.07	2.00, 2.01	1.18	−4.2	1841 (1855[41])
fcc1	−1.87	2.08, 2.12, 2.12	1.20	−23.2	
hcp1	−1.85	2.09, 2.09, 2.16	1.19	−25.0	
tt1	−1.97	1.83	1.16	−24.9	
tb1	−1.90	2.01, 2.01	1.18	−26.0	
fcc2	not stable: move to tb1				
hcp2	not stable: move to tt1				
blb	−1.94	2.03, 2.03	1.19	−0.1	
1/4 monolayer					
2 et	−2.19	1.84, 1.84	1.16, 1.16	−21.2, 19.6 (15[41]/18[44])	2078, 2021 (2087[33])
2 eb	−2.06	2.02, 2.03, 2.03, 2.03	1.18, 1.18	−20.3, 21.0	1895, 1833
		Un-reconstructed (2 × 1)			
1/4 monolayer					
et	−2.55	1.83 (1.9[48])	1.16 (1.3[48])	0.5 (0.0[44])	2068
eb	−2.27	2.01, 2.01	1.18	−1.3	1862
lb	not stable: move to st				
fcc1	not stable: move to eb				
1/2 monolayer					
2 et	−2.27	1.84, 1.84 (1.9[48])	1.16, 1.16 (1.3[48])	−16.3, 18.9 (20[47]/22[44]/25[40,46])	2089, 2004 (2094[33])
2 eb	−2.09	2.02, 2.02, 2.03, 2.03	1.18, 1.18	−18.1, 19.4	1922. 1836 (1915[42])

[a] Adsorption energy per CO molecule. [b] Tilt angle stands for the angle of the C−O axis from the (110) normal. [c] For experimental values in the literature, exact determination of coverage is difficult, and usually exposures are only available.

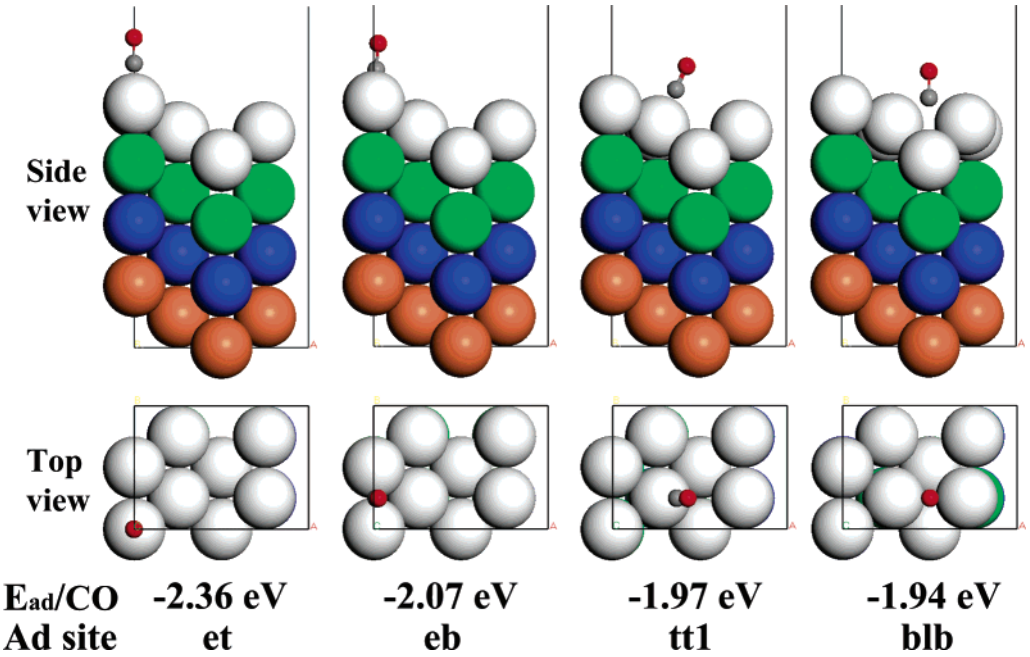

Figure 6. Typical adsorption structures of CO on Pt(110) at the coverage of 1/8 monolayer in the reconstructed (2 × 2) unit cell.

They have proposed a structure containing CO at three adsorption sites; the atop sites on the [110] atomic rows (edge atoms in Figure 2) and atop and bridges sites on the (111) microfacets. This model has been further developed in an X-ray photoelectron diffraction (XPD) study from the same laboratory.[44]

We have calculated adsorption energies and structures of CO on Pt(110) with two different surface models: metastable reconstructed missing row (2 × 2) and un-reconstructed (2 × 1) unit cells (c(8 × 4) structure is not investigated in the present work due to its large unit cell). The calculated adsorption energies and structures are listed in Table 3 (quasi 4-fold hollow sites at the bottom are not investigated because 4-fold hollow sites are less stable, as shown in previous sections for Pt(100) and Pt(410)). Typical optimized adsorption structures for CO on Pt(110) are shown in Figures 6−8. The most favorite adsorption on the reconstructed missing row (1 × 2) phase at 1/8 monolayer occurs at the et site with $E_{ad} = -2.36$ eV (for abbreviation of adsorption sites, see the caption of Figure 2). The energy difference from the second favorite site of eb is 0.29 eV. The third favorite adsorption occurs at the tt1 site with $E_{ad} = -1.97$ eV. Adsorption energies for the tt1 and tb1 sites are quite similar to those for the atop and bridge sites on Pt-(111),[6] which is consistent with the fact that the tt1 and tb1 sites are located on the (111) microfacets of the Pt(110)-(1 × 2) surface. The blb site is locally stable and is the fourth favorite site with $E_{ad} = -1.94$ eV, which is more stable than the 3-fold

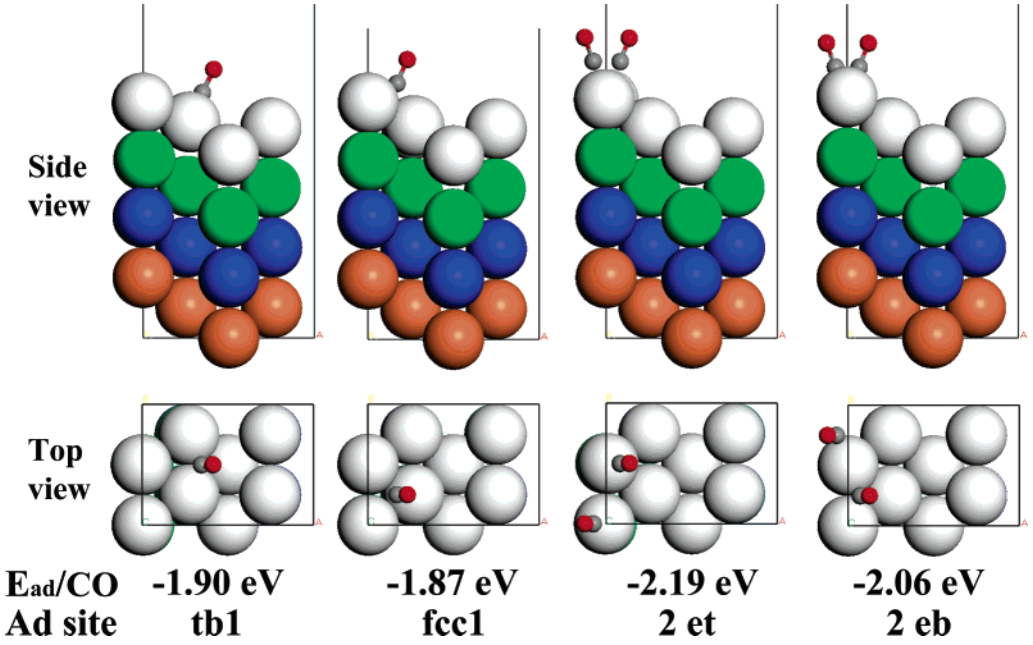

Figure 7. Typical adsorption structures of CO on Pt(110) at the coverages of 1/8 and 1/4 monolayer in the reconstructed (2 × 2) unit cell.

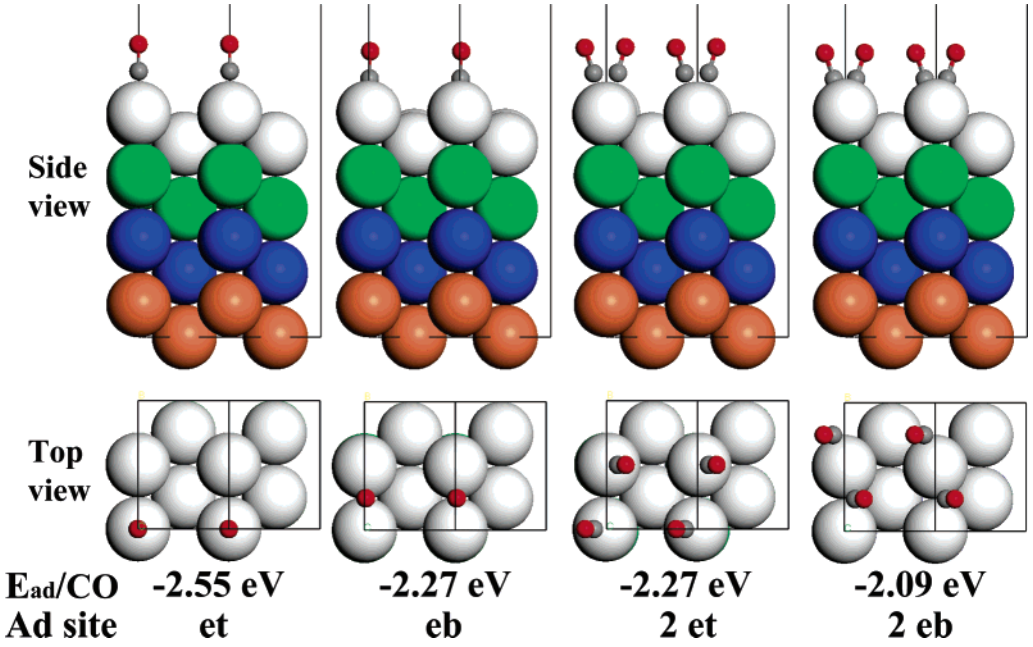

Figure 8. Typical adsorption structures of CO on Pt(110) at the coverages of 1/4 and 1/2 monolayer in the un-reconstructed (2 × 1) unit cell. Two unit cells are shown to compare with adsorption structures in the reconstructed (2 × 2) unit cell.

hollow sites on the (111) microfacets (fcc1, −1.87 eV; hcp1, −1.85 eV). The two Pt atoms attaching to CO move closer together considerably. The Pt−C distances for the blb CO species become similar to those for the tb1 species. King and co-workers have measured the adsorption heat of CO on Pt(110) calorimetrically.[45] The initial heat of adsorption at 300 K is 1.90 eV, declining monotonically to 1.51 eV at 0.25 monolayer and 1.30 eV at the saturation coverage of 0.44 monolayer (it should be noted that in the papers of King and co-workers[3,4,18,33,40−42,45] a differently defined monolayer is used, and their defined monolayer equals twice that of ours in the present work). Our calculated adsorption energies are a little large in comparison with the experimental results because of the tendency of overestimation in the DFT methods. The tilt angle of the adsorbed CO at the et site is calculated as 0.4° from the surface normal. According to the ARUPS experiments,[40] adsorbed CO at the atop site is upright at the low coverage. Our calculation result is in good agreement with the experimental result.

The most favorite adsorption on the reconstructed missing row (1 × 2) phase at 1/4 monolayer also occurs at the et site with $E_{ad} = -2.19$ eV/CO. The energy difference from the second favorite site of eb is 0.13 eV/CO. The two atop CO species in the (2 × 2) unit cell tilt alternately, and the tilt angles are calculated as −21.2 and +19.6° from the surface normal in opposite directions, respectively, which are again in good agreement with the ARUPS result of ca. 15° [41] and the XPD result of 18° [44] in opposite directions at the high CO coverage.

For the un-reconstructed (1 × 1) phase, the most favorite adsorption occurs at the et site with $E_{ad} = -2.55$ eV at 1/4

monolayer. The energy difference from the second favorite site of eb is 0.28 eV. The lb and fcc1 sites become unstable for the un-reconstructed (1 × 1) phase, and the CO molecules move to the et and eb sites, respectively. The tilt angles of the adsorbed CO at the et and eb sites are calculated as +0.5 and −1.3° from the surface normal, respectively. According to the XPD experiment,[44] CO adsorbs at atop sites perpendicularly on the Pt(110)-(1 × 1) surface for unsaturated coverages, which agrees well with the present calculation result.

The most favorite adsorption at 1/2 monolayer for the un-reconstructed (1 × 1) phase also occurs at the et site with E_{ad} = −2.27 eV/CO. The energy difference from the second favorite site of eb is 0.16 eV/CO. The two atop CO molecules in the (2 × 1) unit cell tilt alternately, and the tilt angles are −16.3 and +18.9° from the surface normal in opposite directions, respectively, which are again in good agreement with the ARUPS results of ca. 25 [40,46] or 20° [47] and the XPD result of 22° [44] in opposite directions at the saturation coverage. The structure of 2et CO species at 1/2 monolayer corresponds to the ordered (2 × 1)-p1g1-CO structure, and does more exactly to the (2 × 1)-p2mg structure as confirmed by Nowicki et al.[44] since the tilt of CO is along the [001] azimuth. This ordered, high-coverage structure can only be obtained by annealing the substrate at ca. 600 K and cooling in a CO ambient of 10^{-7} mbar, or by preadsorption of NO at 300 K and subsequent reaction with CO, or by CO adsorption on a metastable and "clean" (1 × 1) surface. The inability to form the ordered (2 × 1)-p1g1 (or p2mg) structure at room temperature has been attributed to the imperfect lifting of the reconstruction.

In all the cases, the Pt−C and C−O distances of the most favorite adsorption site of et are calculated as 1.83−1.84 and 1.16 Å, respectively. They are in good agreement with those of the experimental ones for CO on Pt(111) by LEED[34] (Pt−C distance, 1.85 ± 0.1 Å; C−O distance, 1.15 ± 0.05 Å). Schwegmann et al. have performed a RHEED experiment[48] and estimated the Pt−C and C−O distances as 1.9 ± 0.1 and 1.3 ± 0.1 Å, respectively, for the disordered CO/Pt(110) system, whose disorder prevents the use of techniques that rely on periodic structures, especially LEED I/V analysis. They are a little longer than our calculation results and those for CO on Pt(111) by LEED, although the difference is within the error bars of the RHEED experiment.

Comparing the adsorption energies of CO on the et site of the Pt(110) surface at 1/4 monolayer between the reconstructed missing row (2 × 2) and un-reconstructed (2 × 1) unit cells, the adsorption energy in the un-reconstructed (2 × 1) unit cell is 0.36 eV/CO larger than that in the reconstructed missing row (2 × 2) unit cell. On the other hand, we have found that without CO adsorption the reconstructed (2 × 2) unit cell is more stable than the un-reconstructed (2 × 1) unit cell by 0.17 eV/(2 × 1) surface unit cell. Therefore, the adsorption of CO at 1/4 monolayer should lead to lifting of Pt(110) surface to the un-reconstructed phase because the total energy is more stable by 0.19 eV/(2 × 1) unit cell for the unreconstructed phase than the reconstructed phase.

Ge and King have performed DFT calculation of CO on Pt(110) with pseudopotential and plane-wave basis set.[18] The most stable adsorption site at 1/4 monolayer on the unreconstructed surface (it should be noted that the differently defined monolayer is used by King and co-workers, as mentioned above) is reported as the atop site on the edge with E_{ad} = −2.153 eV, but the energy difference from the bridge site is only 0.024 eV. Their adsorption energy is also overestimated in comparison with the experimental results, the same as our results. The Pt−C and C−O distances are calculated as 1.847 and 1.157 Å, respectively, which are in good agreement with our results (1.84 and 1.16 Å). On the other hand, the most favorable adsorption site at 1/8 monolayer on the reconstructed surface is reported as the bridge site with E_{ad} = −2.112 eV, and the atop site is less stable by 0.006 eV. This result contradicts the experimental results observed by King and co-workers[33,40−42] and our calculation results. The Pt−C and C−O distances for the atop site are calculated as 1.845 and 1.154 Å, respectively, which is also consistent with our calculation results. By means of another plane-wave-based DFT code, Nørskov and co-workers[49] also have found that the most stable adsorption site is the bridge site on edge but not the atop site for the Pt(110)-(1 × 2) surface and that the energy difference between the two sites is ca. 0.05 eV. Furthermore, they have not reported such important information as bond lengths of adsorbed CO, distances between Pt and C atoms, and tilt angles of the C−O axis.

Vibrational frequencies have been calculated for CO species at the et and eb sites (see Table 3). With an increase in the coverage from 1/8 to 1/2 monolayer, the C−O stretching frequency of the et species increases slightly from 2055 to 2089 cm^{-1}, which agrees well with the experimental shift from 2080 to 2117 cm^{-1},[42] or from 2058 to 2099 cm^{-1}.[33] For the eb species, the calculated frequency increases from 1841 to 1922 cm^{-1}. Experimentally, the bridge species is observed only with HREELS (but not with RAIRS) at 1855 cm^{-1} by adsorption on the Pt(110)-(1 × 2) surface at lower temperature[41] or 1915 cm^{-1} upon partial desorption from the (2 × 1)-p1g1 structure.[42] The calculated frequency corresponds well to the experimental one for the bridge species as well as the atop species, which confirms the assignment of adsorption sites.

4. Conclusion

Adsorption of CO on Pt(100), Pt(410), and Pt(110) surfaces has been investigated by density functional theory (DFT) method (periodic DMol[3]) at the generalized gradient approximation (GGA) level with full geometry optimization and without symmetry restriction. Adsorption energies, structures, and vibrational frequencies of CO on these surfaces are studied by considering multiple possible adsorption sites and comparing them with the experimental data. Calculated C−O stretching frequencies agree well with experimental ones, and precise determination of adsorption sites can be carried out. The same site preference as inferred experiments is obtained for all the surfaces. For Pt(100), CO adsorbs at the bridge site at low coverage, but the atop site becomes most favorable for the *c*(2 × 2) structure at 1/2 monolayer. The energy difference between the atop and bridge sites is only 0.03 eV/CO, so the atop and bridge domains are populated simultaneously as suggested by RAIRS experiments. For Pt(410) (stepped surface with (100) terrace and (110) step), CO adsorbs preferentially at the atop site on step edge at 1/4 monolayer, but CO populates also at other atop and bridge sites on the (100) terrace at 1/2 monolayer. The multiple possible adsorption sites probably correspond to the multiple states in the TPD spectra for CO desorption. For Pt(110), CO adsorbs preferentially at the atop site on the edge for both the reconstructed missing row (1 × 2) surface and the un-reconstructed (1 × 1) surface. When adjacent sites along the edge row begin to be occupied, the CO molecules tilt alternately by ca. 20° from the surface normal in opposite directions for both the (1 × 2) and (1 × 1) surface. The un-reconstructed (1 × 1) surface is more stable than the reconstructed (1 × 2) surface when CO adsorbs on the surface.

Supporting Information Available: Other optimized adsorption structures of CO on Pt(410) and Pt(110)-(1 × 2) (PDF). This material is available free of charge via the Internet at http://pubs.acs.org.

References and Notes

(1) Somorjai, G. A. *Introduction to Surface Chemistry and Catalysis*; Wiley: New York, 1994.
(2) Matsushima, T. *Surf. Sci. Rep.* **2003**, *52*, 1.
(3) Brown, W. A.; Kose, R.; King, D. A. *Chem. Rev.* **1998**, *98*, 797.
(4) Ge, Q.; Kose, R.; King, D. A. *Adv. Catal.* **2000**, *45*, 207, and references therein.
(5) Feibelman, P. J.; Hammer, B.; Nørskov, J. K.; Wagner, F.; Scheffler, M.; Stumpf, R.; Watwe, R.; Dumesic, J. *J. Phys. Chem. B* **2001**, *105*, 4018.
(6) Orita, H.; Itoh, N.; Inada, Y. *Chem. Phys. Lett.* **2004**, *384*, 271.
(7) McEwen, J.-S.; Payne, S. H.; Kreuzer, H. J.; Kinne, M.; Denecke, R.; Steinrück, H.-P. *Surf. Sci.* **2003**, *545*, 47.
(8) Shah, V.; Li, T.; Baumert, K. L.; Cheng, H.; Sholl, D. S. *Surf. Sci.* **2003**, *537*, 217.
(9) Karmazyn, A. D.; Fiorin, V.; Jenkins, S. J.; King, D. A. *Surf. Sci.* **2003**, *538*, 171.
(10) Mason, S. E.; Grinberg, I.; Rappe, A. M. *Phys. Rev. B* **2004**, *69*, 161401.
(11) Orita, H.; Itoh, N.; Inada, Y. *Surf. Sci.* **2004**, *571*, 161.
(12) Behm, R. J.; Thiel, P. A.; Norton, P. R.; Ertl, G. J. *Chem. Phys.* **1983**, *78*, 7473.
(13) Martin, R.; Gardner, P.; Bradshaw, A. M. *Surf. Sci.* **1995**, *342*, 69.
(14) Yeo, Y. Y.; Vattuone, L.; King, D. A. *J. Chem. Phys.* **1995**, *104*, 3810.
(15) Comrie, C. M.; Lambert, R. M. *J. Chem. Soc., Faraday Trans. 1* **1976**, *72*, 1659.
(16) Fery, P.; Moritz, W.; Wolf, D. *Phys. Rev. B* **1988**, *38*, 7275.
(17) Hammer, B.; Nielsen, O. H.; Nørskov, J. K. *Catal. Lett.* **1997**, *46*, 31.
(18) Ge, Q.; King, D. A. *J. Chem. Phys.* **1999**, *111*, 9461.
(19) Ge, Q.; Desai, S.; Neurock, M.; Kourtakis, K. *J. Phys. Chem. B* **2001**, *105*, 9533.
(20) Creighan, S. C.; Mukerji, R. J.; Bolina, A. S.; Lewis, D. W.; Brown, W. A. *Catal. Lett.* **2003**, *88*, 39.
(21) Delley, B. *J. Chem. Phys.* **1990**, *92*, 508.
(22) Delley, B. *J. Phys. Chem.* **1996**, *100*, 6107.
(23) Delley, B. *J. Chem. Phys.* **2000**, *113*, 7756.
(24) Perdew, J. P.; Burke, K.; Ernzerhof, M. *Phys. Rev. Lett.* **1996**, *77*, 3865.
(25) Delley, B. *Int. J. Quantum Chem.* **1998**, *69*, 423.
(26) Delley, B. *Phys. Rev. B* **2002**, *66*, 155125.
(27) Gil, A.; Clotet, A.; Ricart, J. M.; Kresse, G.; García-Hernández, M.; Rösch, N.; Sautet, P. *Surf. Sci.* **2003**, *530*, 71.
(28) *CRC Handbook of Chemistry and Physics*, 81st ed.; Lide, D. R., Ed.; CRC Press: Boca Raton, FL, 2000.
(29) Kurth, S.; Perdew, J. P.; Blaha, P. *Int. J. Quantum Chem.* **1999**, *75*, 889.
(30) Orita, H.; Nakamura, I.; Fujitani, T. *Surf. Sci.* **2004**, *571*, 102.
(31) Morgan, A. E.; Somorjai, G. A. *Surf. Sci.* **1968**, *12*, 405.
(32) Morgan, A. E.; Somorjai, G. A. *J. Chem. Phys.* **1969**, *51*, 3309.
(33) Sharma, R. K.; Brown, W. A.; King, D. A. *Surf. Sci.* **1998**, *414*, 68.
(34) Ogletree, D. F.; van Hove, M. A.; Somorjai, G. A. *Surf. Sci.* **1986**, *173*, 351.
(35) Park, Y. O.; Masel, R. I.; Stolt, K. *Surf. Sci.* **1983**, *131*, L385.
(36) Park, Y. O.; Banholzer, W. F.; Masel, R. I. *Surf. Sci.* **1985**, *155*, 341.
(37) Banholzer, W. F.; Parise, R. E.; Masel, R. I. *Surf. Sci.* **1985**, *155*, 653.
(38) Luo, J. S.; Tobin, R. G.; Lambert, D. K.; Fisher, G. B.; DiMaggio, C. L. *Surf. Sci.* **1992**, *274*, 53.
(39) Mukerji, R. J.; Bolina, A. S.; Brown, W. A. *Surf. Sci.* **2003**, *527*, 198.
(40) Hofmann, P.; Bare, S. R.; King, D. A. *Surf. Sci.* **1982**, *117*, 245.
(41) Hofmann, P.; Bare, S. R.; King, D. A. *Phys. Scr.* **1983**, *T4*, 118.
(42) Bare, S. R.; Hofmann, P.; King, D. A. *Surf. Sci.* **1984**, *144*, 347.
(43) Freyer, N.; Kiskinova, M.; Pirug, G.; Bonzel, H. P. *Appl. Phys. A* **1986**, *39*, 209.
(44) Nowicki, M.; Emundts, A.; Pirug, G.; Bonzel, H. P. *Surf. Sci.* **2001**, *478*, 180.
(45) Wartnaby, C. E.; Stuck, A.; Yeo, Y. Y.; King, D. A. *J. Phys. Chem.* **1996**, *100*, 12483.
(46) Bare, S. R.; Griffiths, K.; Hofmann, P.; King, D. A.; Nyberg, G. L.; Richardson, N. V. *Surf. Sci.* **1982**, *120*, 367.
(47) Rieger, D.; Schnell, R. D.; Steinmann, W. *Surf. Sci.* **1984**, *143*, 157.
(48) Schwegmann, S.; Tappe, W.; Korte, U. *Surf. Sci.* **1995**, *334*, 55.
(49) Thostrup, P.; Christoffersen, E.; Lorensen, H, T.; Jacobsen, K. W.; Besenbacher, F.; Nørskov, J. K. *Phys. Rev. Lett.* **2001**, *87*, 126102.